Article

Exploring the Possibility of Using Ionic Copolymer Poly (Ethylene-*co*-Methacrylic) Acid as Modifier and Self-Healing Agent in Asphalt Binder and Mixture

Yuefeng Zhu [1,2,3], Reyhaneh Rahbar-Rastegar [4], Yanwei Li [5,6], Yaning Qiao [7],* and Chundi Si [1,2,3],*

1   State Key Laboratory of Mechanical Behavior and System Safety of Traffic Engineering Structures, Shijiazhuang Tiedao University, Shijiazhuang 050043, China; yuefengzhu@stdu.edu.cn
2   Key Laboratory of Traffic Safety and Control of Hebei Province, Shijiazhuang 050043, China
3   School of Traffic and Transportation, Shijiazhuang Tiedao University, Shijiazhuang 050043, China
4   Lyles School of Civil Engineering, Purdue University, West Lafayette, IN 47907, USA; rrahbar@purdue.edu
5   Hebei Provincial Communications Planning and Design Institute, Shijiazhuang 050043, China; liyanwei69@vip.sina.com
6   Research and Development Center of Transport Industry of Technologies, Materials and Equipments of Highway Construction and Maintenance, Shijiazhuang 050043, China
7   School of Mechanics and Civil Engineering, China University of Mining and Technology, Xuzhou 221116, China
*   Correspondence: yaning.qiao@cumt.edu.cn (Y.Q.); sichundi@stdu.edu.cn (C.S.);
    Tel.: +86-185-1097-5708 (Y.Q.); +86-159-3266-1937 (C.S.)

check for updates

Abstract: It is well-accepted that the ionic copolymer poly (ethylene-*co*-methacrylic) acid (also named EMAA) is one type of self-healing material. This particular capability has great potential for extending the service life of infrastructures. In order to improve the rheological, mechanical, and self-healing properties of asphalt binder and asphalt mixtures, EMAA and styrene butadiene rubber (SBR) were selected as the additives. In this study, the effects of EMAA and SBR on the performance of bitumen and asphalt mixtures were examined and characterized using various parameters including rheological indices, Glover–Rowe parameter, ductility self-healing rate, fluorescence microscopy, and scanning electron microscope (SEM) test on binders, and different testing methods such as complex modulus, thermal stress-restrained specimen test (TSRST), disk-shaped compact tension (DCT), and fatigue–healing–fatigue test on the mixtures. The results showed that EMAA can significantly improve the stiffness and self-healing capacity of virgin and SBR modified binders and mixtures. Moreover, the cracking resistance of EMAA/SBR compound modified binder and mixture showed a significant improvement. However, EMAA is not recommended to be added as a modifier to virgin binders and mixtures due to its poor cracking resistance. Some novel tests and parameters mentioned in this paper are recommended for characterizing binders and mixtures in the future.

Keywords: poly(ethylene-co-methacrylic) acid; SBR; self-healing; stiffness; relaxation; fracture strain tolerance

1. Introduction

Asphalt binder has been used for many years in paving and roofing constructions because of its great viscoelastic properties [1]. However, with the influence of traffic loading and environmental conditions, the relaxation capability and flexibility of asphalt mixtures gradually decline resulting in more ageing and lower cracking resistance, and this phenomenon is more obvious for virgin asphalt or reclaimed asphalt. To alleviate this problem, some additive agents were selected to be added

to asphalt binders as modifiers to improve the mechanical and rheological abilities of asphalt [2]. There are different types of modifiers such as polymers, minerals, acids, etc., but among them, the styrene-butadiene rubber (SBR) has shown a great potential to increase the thermal cracking resistance of virgin binder. Becker et al. found that SBR modified asphalt could significantly improve the viscosity and ductility of virgin asphalt, in addition to enhance the cracking resistance of asphalt mixture [3]. However, SBR modified asphalt is more prone to aging due to its butadiene-rich structure. Moreover, SBR-modified asphalt and asphalt mixture were susceptible to high-temperature damage because of the modification method, which results in poor high-temperature stability and compatibility [4]. Therefore, in order to obtain a comprehensive performance, as well as the high stability of asphalt binder, it is necessary to investigate more effective additives in combination with SBR.

The self-healing capability of asphalt has been investigated in several researches. It has been proved that self-healing has the potential to prolong the serviceability of asphalt concrete [5–7]. In general, the research of self-healing mechanism is still a hot topic. Several methods and models were used to fully understand the self-healing phenomenon, such as molecular diffusion healing model, surface energy healing model, capillary flow healing model [8]. Based on the research by Qiu et al. [9], the self-healing of asphalt materials was influenced by many factors, including rest time, temperature, binder properties, damage level, and material modifications. The healing process at the ambient temperature is very slow, and it is difficult to healing the micro cracks and other damages during the service life of asphalt concrete. Therefore, various external intervention methods were performed to speed up the healing process, such as heating the asphalt concrete by electromagnetic induction [10,11], microwave induction [12,13], and mixing microcapsules containing healing agent [14,15] in asphalt concrete.

In addition, the concept of self-healing comes from the natural and biological phenomena, which can help the organisms recover, repair the cracks, and finally lengthen the span of life. Nowadays, some novel self-healing materials including hollow fibers, nanoparticles, and ionomers were used in functional composite materials (such as polymer and asphalt) [16]. The ionomer poly(ethylene-*co*-methacrylic) acid (EMAA) has shown a great potential for the self-healing reinforcement of asphalt materials. Meure et al. [17] studied self-healing efficiency and mechanism of EMAA in epoxy resin and found that EMAA has different healing process than the other repairable polymer systems. Meure et al. [18] reported that the cracks in carbon fiber–epoxy laminates can achieve self-healing by using EMAA fibers or particles. In addition, the self-healing efficiency by using EMAA is higher than using the microcapsule method. Pingakararwat et al. [19] confirmed that adding EMAA in carbon–epoxy laminates is an effective way to prevent the fatigue and static cracks. In another study, Wang et al. [20] investigated the compatibilizing ability of EMAA on polyvinyl chloride (PVC)/polypropylene (PP) composite materials. The results showed that EMAA had better compatibilizing ability than ethylene-vinyl acetate copolymer (EVA) and low-density polyethylene (LDPE). Therefore, it is required to explore the compatibility effects of EMAA on polymer-modified asphalt, such as SBR-modified asphalt or SBS-modified asphalt, which might improve the comprehensive performance of polymer modified asphalt and its mixture.

In consideration of the above situation, the main idea of this study is to explore the possibility of using EMAA as modifier and self-healing agent in asphalt materials. The rheological, mechanical, and self-healing abilities of EMAA added to asphalt materials have been evaluated using traditional as well as some newly developed test methods. Also, proper parameters are selected to better assess the properties of binders and mixtures.

2. Materials

2.1. Virgin Binder and Aggregate

The virgin binder used in this study was Shell 70[#] road asphalt binder. The main physical properties of virgin binder are shown in Table 1. The coarse and fine aggregates were basalts and limestone, respectively, and the limestone powder was used as mineral filler. The physical properties of coarse and fine aggregates and mineral filler are presented in Table 2.

Table 1. Physical properties of base asphalt.

Test Properties		Results	Requirement
Penetration (25 °C, 100g, 5 s)/0.1 mm		74.9	60~80
Softening point/°C		46.7	≥46
Ductility (10 °C)/cm		68.5	≥15
Rolling thin film oven (RTFO)	Mass loss/%	0.60	≤0.80
	Penetration ratio/%	71.5	≥61.0
	Ductility (10 °C)/cm	9.8	—

Table 2. Physical properties of aggregate and filler.

Test Properties		Results	Requirement
Coarse aggregate	Crushed value/%	11.8	≤26
	Los Angeles wear value/%	10.6	≤28
	Polished stone value/PSV	43	≥42
Fine aggregate	Apparent relative density	2.679	≥2.50
	Angularity/s	42.7	≥30
Filler	Apparent density/(g·cm^{-3})	2.761	≥2.50
	Water content/%	0.4	≤1

2.2. Modifiers

The basic properties of SBR, which is a white solid powder, are shown in Table 3. EMAA was obtained from Dongguan, China, and the origin is DuPont Company, USA. The physical properties of EMAA are presented in Table 4. Figure 1 shows the shape and appearance of EMAA and SBR used in this study.

Table 3. Basic properties of styrene butadiene rubber (SBR).

Test Properties	Values	Standards
Particle size/mesh	<80	GB/T8656
Tensile strength/MPa	22	GB/T8656
Styrene content/%	17~19	GB/T8658
Mooney viscosity/(Pa·s)	68	GB/T8657

Table 4. Basic properties of poly(ethylene-*co*-methacrylic) acid (EMAA).

Test Properties	Values	Standards
Density/(g/cm^3)	0.93	ASTM D792
Vicat softening temperature/°C	65.0	ASTM D1525
Melting point/°C	95	ASTM D3418
Tensile strength/MPa	32	ASTM D1238

Figure 1. Shape and appearance of EMAA and SBR.

2.3. Binder Preparation

Four types of binders were evaluated in this study, including virgin binder, SBR-modified binder, EMAA-modified binder, and EMAA–SBR (compound)-modified binder. The modified asphalt binders were prepared as follows:

(1) SBR-modified asphalt

First, the virgin binder was heated up to 155 ± 5 °C. Then, based on the group results [21], the optimum amount of SBR (3% of total binder weight) was added to the virgin binder and stirred for 20 min. After that, the binder was sheared at 5000 r/min for 30 min. During this process, the temperature was kept constant.

(2) EMAA/SBR compound-modified asphalt

The virgin binder was heated up to 155 ± 5 °C. Then, a proper amount (1%, 2%, 3%, 4%, 5%, or 6% by total weight) of EMAA was added to the binder and stirred for 30 min. After that, the binder was sheared at 5000 r/min for half an hour. Finally, 3% SBR was added and continuously sheared for another 30 min.

In this study, the contents of EMAA were preliminary selected as 1%, 2%, 3%, 4%, 5%, and 6% by total weight of the binder specimen. Various important material parameters, including softening point, equivalent softening point, kinematic viscosity, and ductility (10 °C), in accordance with JTG E 20-2011 [22], were used to determine the optimum dosage of EMAA. The physical properties of modified binders with different EMAA contents are shown in Table 5.

Table 5. Physical properties of EMAA/SBR compound-modified asphalt.

Binder Type	Softening Point/°C	Equivalent Softening Point (T800)/°C	Kinematic Viscosity (135 °C)/Pa·s	Ductility (10 °C)/cm
3%SBR	57.5	53.4	1.33	>100
1% EMAA + 3% SBS	65.5	56.9	1.45	>100
2% EMAA + 3% SBS	68.9	59.3	1.58	>100
3% EMAA + 3% SBS	73.2	61.9	1.73	>100
4% EMAA + 3% SBS	74.3	63.2	1.82	>100
5% EMAA + 3% SBS	75.0	64.3	1.89	92.3
6% EMAA + 3% SBS	75.5	64.8	1.93	76.5

It can be seen in Table 5 that after adding EMAA, the softening point, equivalent softening point (T800), and kinematic viscosity (135 °C) of asphalt increased. This indicates that EMAA can improve the high-temperature stability of SBR-modified asphalt. The reason might be that EMAA promoted the stability and compatibility of SBR-modified asphalt, and also the methyl branched chain on EMAA could increase the viscosity of asphalt. However, as the content of EMAA increased from 1% to 6%, the ductility (10 °C) decreased from above 100 to 76.5 (cm). Thus, the critical point could be at 4% EMAA. Moreover, when the content of EMAA was more than 4%, the increasing rate of softening point,

equivalent softening point (T800), and kinematic viscosity (135 °C) gradually decreased. For economic considerations, 4% of EMAA was chosen in this study.

(3) Preparation of EMAA-modified asphalt

Asphalt with 4% EMAA was also produced. The procedures were the same as mentioned previously.

Four kinds of binders, including virgin binder, virgin binder + 3% SBR, virgin binder + 4% EMAA + 3% SBR, and virgin binder + 4% EMAA, were recorded as virgin, 3%SBR, 4%EMAA/3%SBR, and 4%EMAA for simplicity.

2.4. Mixture Preparation

The mix design was followed by the Technical Specification for Construction of Highway Asphalt Pavement (JTGF40-2004) [23]. The mixture gradation was determined based on the dense gradation, and a typical gradation of AC-13 was selected for all the mixtures, as shown in Figure 2. The asphalt-aggregate ratio was determined by Marshell test results. The target air void of all the mixtures was controlled at 3.5–4%. The optimum asphalt–aggregate ratio of virgin mixture, 4%EMAA-modified asphalt mixture, 3%SBR-modified asphalt mixture, and 4%EMAA/3%SBR compound-modified asphalt mixture were 4.0%, 4.2%, 4.5%, and 4.6%, respectively.
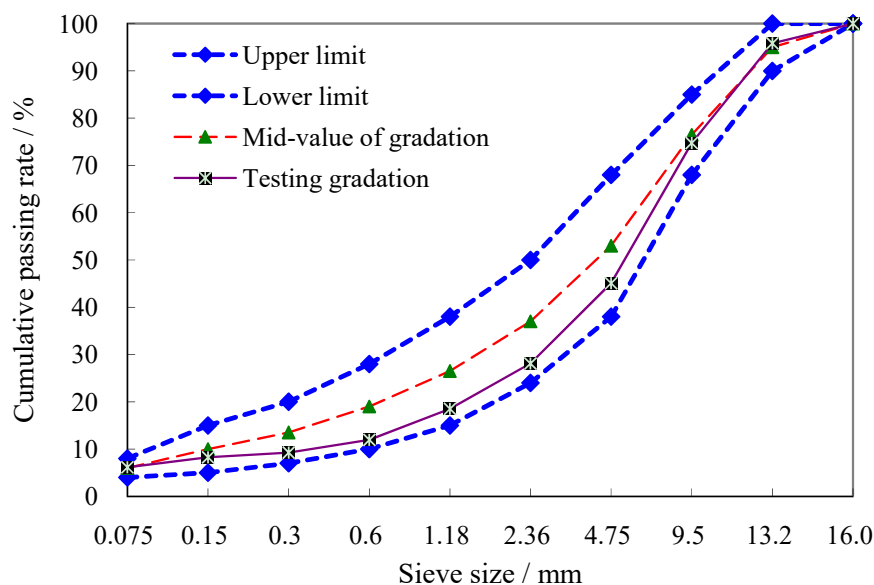

Figure 2. Gradation curve of AC-13.

3. Methodology

3.1. Binder Testing and Analysis

As mentioned earlier, binder testing and analysis were conducted on four different types of binders. Dynamic shear rheometer (DSR) was used to study the rheological properties of binders. The self-healing property of binders was measured using ductility test and the interaction mechanism of binders was studied using fluorescence microscopy test.

3.1.1. Binder Master Curves and Glover-Rowe Parameter

According to AASHTO T315, the binder specimens with 25 mm diameter were tested at the temperatures of 5, 15, 25, and 35 °C and loading frequencies within a strain range from 0.005 to 0.02. The complex modulus (G^*) and phase angle (δ) of binders were measured at testing frequencies and temperatures, and the binder master curves were generated at 25 °C reference temperature, using the time-temperature superposition principle, based on the Christensen–Anderson–Marasteanu Model (CAM) [24].

Glover et al. [25] developed the rheological parameter, $G'/(\eta'/G')$, as an indicator of cracking potential of binders. Later, Rowe [26,27] simplified the Glover parameter, as Glover–Rowe (G-R) parameter, to evaluate the binder cracking properties. G-R parameter can be calculated from $|G^*| \cdot (\cos\delta)^2/\sin\delta$, at temperature–frequency combination of 15 °C and 0.005 rad/s.

3.1.2. Ductility Test

The ductility test was used to investigate the self-healing ability of binders. The testing procedure is as follows: (1) Six ductility test samples for each type of binder were prepared based on the JTG E 20-2011 [22] specification; (2) a 5 mm depth artificial crack was cut in the middle of binder specimens at the room temperature (about 25 °C), as shown in Figure 3; (3) six samples were divided in two comparative groups for each type of binder, 10 °C ductility test was conducted on three samples directly, and three samples were tested after 24 h at the room temperature (about 25 °C). For quantitative analysis, the healing rate (*D*) was used to evaluate the healing capacity of different binders, and the calculation of *D* is shown in Equation (1).

$$D = \frac{L_{\text{healed}} - L_{\text{original}}}{L_{\text{original}}} \times 100\% \tag{1}$$

where L_{original} is the ductility of the fractured sample without time interval and L_{healed} is the ductility of the fractured sample with 24 h interval.
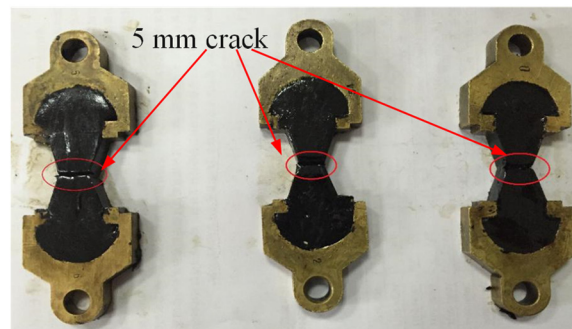
Figure 3. Fracture samples for self-healing ductility test.

3.1.3. Fluorescence Microscopy Test

The morphologies of different binders were observed using fluorescence microscopy equipped with Canon 6D digital camera. Observation was made at room temperature with a magnification of 100. More details of test sample preparation can be found in literature [28].

3.1.4. Scanning Electron Microscope (SEM) Test

The micro morphologies of virgin, SBR-modified binder and EMAA/SBR compound-modified binder were tested on SEM test device manufactured by Netherland. The stability and anti-fracture property of different binders were studied based on the micro morphologies.

3.2. Mixture Testing

Mixture evaluation methods are discussed in this section, in supplement to binder characterization testing. To investigate the characteristics of different asphalt mixtures, four testing methods were performed, including complex modulus test, thermal stress-restrained specimen test (TSRST), disk-shaped compact tension (DCT), and fatigue–healing–fatigue test. Detailed descriptions for the tests are provided below.

3.2.1. Complex Modulus Test

Complex modulus test is a test method to evaluate the viscoelastic properties of asphalt mixtures following AASHTO TP79-15 [29]. An asphalt mixture performance tester (AMPT) was used to test the specimens, and dynamic modulus ($|E*|$) and phase angle (δ) were measured as two important viscoelastic characteristics of mixtures. The testing was conducted on three replicates for each mixture. Standard specimen with 150 mm high and 100 mm in diameter was tested at 4.4 °C, 21.1 °C, and 37.8 °C and the frequencies of 0.1, 0.5, 1, 5, 10, and 25 Hz. According to the time–temperature superposition principle, a generalized logistic function (Equation (2)) was used to develop the master curve of average dynamic modulus isotherms at the reference temperature of 21.1 °C.

$$\log|E*| = \delta + \frac{\alpha}{\left[1 + \lambda(\exp^{\beta + r(\log \omega_r)})\right]^{1/\lambda}} \tag{2}$$

where $|E*|$ is dynamic modulus (MPa); α, β, γ, δ, and λ are the fitting parameters; and ω_r is reduced frequency (Hz), which can be calculated from frequency multiplied by the shift factor, aT, shown in Equation (3).

$$\log a_T = a_1 T^2 + a_2 T + a_3 \tag{3}$$

where a_1, a_2, and a_3 are shift factor coefficients, and T is temperature.

3.2.2. Thermal Stress-Restrained Specimen Test

The thermal stress-restrained specimen test (TSRST) was used to evaluate the thermal cracking susceptibility of asphalt mixtures. In accordance with AASHTO TP10-93 [30], the asphalt mixtures specimens (54 mm in diameter and 160 mm in height) were placed in an environmental chamber at 5 °C for 2 h. During the test, the temperature decreased at a cooling rate of 10 °C/h to fracture the specimen. Three replicates were tested for each mixture, and the fracture temperature and fracture strength were measured. The lower fracture temperature or the higher fracture strength, the better the low-temperature cracking resistance of asphalt mixture.

3.2.3. Low-Temperature Fracture Test

The thermal stress-restrained specimen test (TSRST) cannot consider the effects of traffic loads and the propagation of cracking over time [31]. To evaluate the low-temperature behavior of asphalt mixture, disk-shaped compact tension (DCT) test, a novel fracture test method, was performed following the ASTM D7313-07 test procedure. DCT testing is controlled to acquire a constant rate of crack mouth opening displacement (CMOD), which is 1 mm/min. Testing temperature was selected to be −18 °C. Typical load-displacement curves obtained from DCT tests are shown in Figure 4. Generally, fracture energy (G_f), as one of the main fracture parameters, can be calculated from the area under the load-CMOD curve. However, it has been found by many researchers (Al-Qadi et al. [32], Zhu et al. [33], and Pérez-Jiménez et al. [34]) that the fracture energy has its drawbacks and could not fully distinguish between the cracking behavior of the mixtures. It can be seen in Figure 4 that the mixture with high peak load (about 3.8 kN) and steep post-peak slope has very close fracture energy value with the mixture exhibiting low peak load (about 2.5 kN) and shallow post-peak slope. Therefore, different indices such as flexibility index (FI), toughness index (TI), and fracture strain tolerance (FST) are proposed to assess the low-temperature properties of asphalt mixtures.
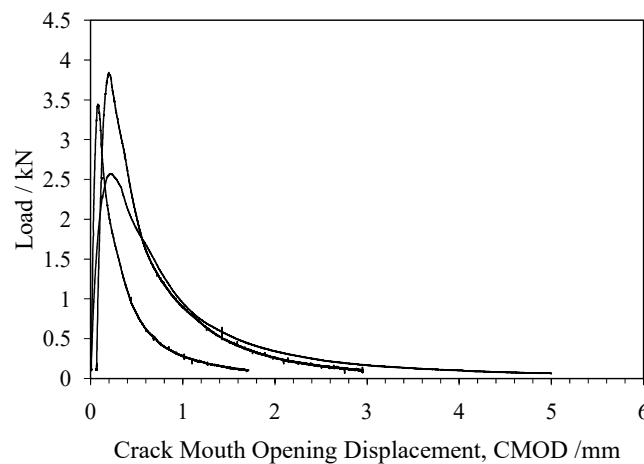
Figure 4. Typical load and crack mouth opening displacement (CMOD) curves.

The FST fracture index was developed by Zhu et al. [33] and showed superiority and lower variability than fracture energy in assessing the low temperature cracking ability of mixtures. The FST parameter can be calculated from Equation (4).

$$\text{FST} = \frac{G_f}{S_f} \tag{4}$$

where G_f is the fracture energy and S_f is the fracture strength of DCT test; the calculation of G_f and S_f are shown in Equations (5) and (6).

$$G_f = \frac{\int_0^{\Delta\text{Final}} F \cdot du}{t \times a} \tag{5}$$

$$S_f = \frac{2F_{\max}(3L - a)}{t \times a^2} \tag{6}$$

where F is the test load during the test, u is the CMOD, ΔFinal is the displacement at the end of the test, t is the thickness of test specimen, a is the crack ligament length, $F_{\max}$ is the peak load, and L is the distance from loading location to specimen's boundary.

3.2.4. Fatigue–Healing–Fatigue Test

The midpoint bending test was conducted to study the fatigue–healing–fatigue behavior of different asphalt mixtures. According to the method T0739-2011 in JTG E20-2011 [22], the sinusoidal load was applied at a frequency of 10 Hz and the testing temperature of 15 °C. The preliminary test was conducted to determine the fatigue life (N_f) at the stress ratio of 0.5. The fatigue life or the number of cycles to failure is defined as the number of cycles when the stiffness modulus drops to 50% of the initial stiffness modulus. The initial stiffness modulus was obtained at the 50th cycle of loading. The fatigue–healing–fatigue testing procedure was as follows. (1) The fatigue test was conducted until 30% fatigue life was achieved; 30% of fatigue life was chosen as the control point of the first fatigue test, which was recorded as N_1; (2) the specimens were placed at room temperature for 24 h as the healing interval; (3) the second fatigue test was conducted on the specimen until the specimen was fully damaged. The number of second fatigue test was record as N_2. The self-healing property of different mixtures can be assessed by the healing rate (H), which can be expressed as follows:

$$H = (N_1 + N_2 - N_f)/N_f. \tag{7}$$

4. Results and Discussion

4.1. Binder Testing Results and Discussion

4.1.1. Complex Modulus Master Curves

The complex shear modulus of different binders is shown in Figure 5. The binder stiffness increases with the inclusion of binder modification. The greatest increase is observed in the binder with 4%EMAA, followed by the 4%EMAA/3%SBR-modified binder. It should be noted that there is no significant difference between the complex modulus of virgin and 3%SBR-modified binder; specifically, the complex modulus values are very close at low frequencies (high temperatures). Interestingly, with 3%SBR added into the 4%EMAA modified asphalt, the stiffness of the 4%EMAA/3%SBR compound-modified binder decreases, indicating that SBR is not able to improve the high-temperature properties of binder.
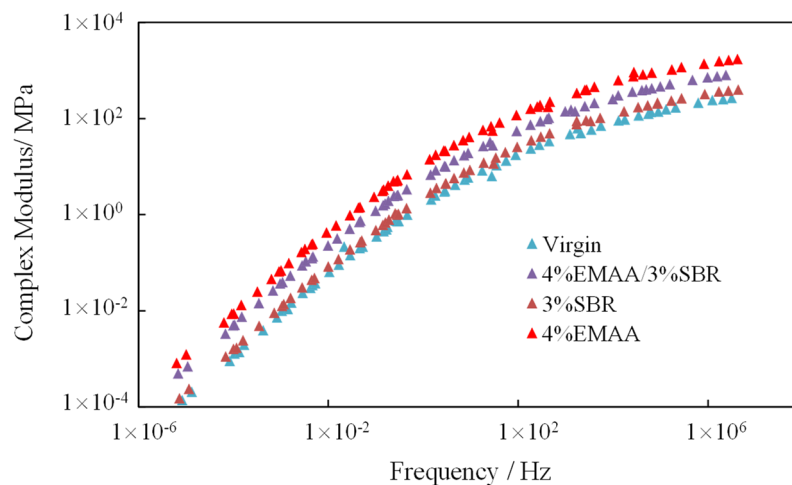
Figure 5. Complex modulus master curves of different binders.

4.1.2. Glover–Rowe Parameter

Figure 6 shows the G-R parameter for different binders. Two boundary curves that indicate the crack onset (G-R = 180 kPa) and significant cracking (G-R = 600 kPa) are added to the Black space diagram. The Black space diagram combines the complex modulus and phase angle to assess both the stiffness and relaxation capability of asphalt materials. With the increase of G* and decrease of phase angle, the asphalt mixtures on field are expected to be more prone to cracking [35]. Therefore, as the G-R values move further up and to the left, the cracking potential of asphalt binders increases. It can be seen in Figure 6 that all the G-R values are lower than the crack onset threshold. However, the cracking potential is expected to be higher for the 4%EMAA-modified binder, as the corresponding G-R parameter becomes closer to the thresholds. The rankings of cracking resistance can be in the following order: EMAA/SBR compound-modified asphalt mixtures > SBR-modified asphalt mixtures > virgin asphalt mixtures > EMAA-modified asphalt mixtures.
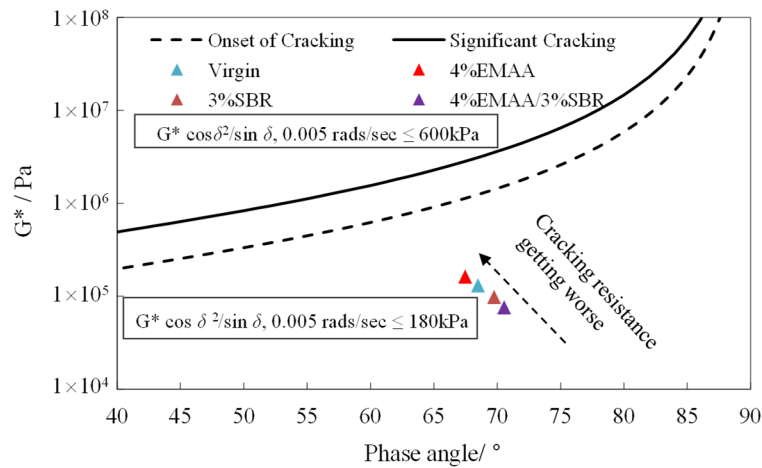
Figure 6. Glover–Rowe parameter analysis in black space for different binders.

4.1.3. Ductility Healing Rate

Table 6 shows the results of ductility test for the different binders. As can be seen in the first row, the average ductility (without 24 h time interval) of virgin binder is 15.2 cm, while the average ductility 4% EMAA-modified binder decreases by 15.8%. This indicates that EMAA has a negative impact on ductility. In contrast, SBR or EMAA/SBR binders show a positive effect on ductility with 6.6% and 33.6% improvement, respectively. After a 24 h time interval, the ductility of all fractured samples increased, indicating a positive effect on self-healing. Another important parameter can be compared between varied binders is healing rate (*D*). It can see in the last row of Table 6 that the binders with EMAA modification show higher healing rate than virgin binder and SBR-modified binder. An interesting observation is that adding the combination of EMAA and SBR improves the self-healing behavior of binder significantly. The healing rate of EMAA/SBR compound-modified binder is 2.04 and 1.53 times than that of virgin binder and SBR-modified binder, respectively. The reason is not only the EMAAs own self-healing capacity, but also is probably because of the complex chemical and physical reactions that occurred among the binder and two kinds of additives.

Table 6. Ductility test results of various binders.

Test Properties	Virgin	4% EMAA	3% SBR	4%EMAA/3%SBR
Average L_{Original}/(cm)	15.2	12.8	16.2	20.3
Average L_{Healed}/(cm)	19.2	18.9	21.9	31.2
D/(%)	26.3	47.7	35.2	53.7

4.1.4. Fluorescence Micrographs

The fluorescence microscopy test was performed to investigate the compatibility and stability among EMAA, SBR, and virgin binder and also provide an explanation of self-healing ductility and rheological results. The fluorescence micrographs of different binders are presented in Figure 7. As illustrated in Figure 7a, there is no pattern observed for virgin binder. After adding 4% EMAA, the morphology of virgin binder is converted to a biphasic structure where the EMAA particles are swollen by absorbing light components and dispersed in the continuous asphalt phase, as shown in Figure 7b. The EMAA particles also present the strip type features. In this situation, the expanded EMAA particles mainly have a significant influence on the viscosity of virgin binder [36]. In addition, there is an obvious interface between EMAA and asphalt, which indicates poor compatibility. However, the SBR particles are distributed like spherical features after the stirring and shearing in virgin binder, as shown in Figure 7c. Compared with EMAA-modified asphalt, the asphalt/SBR system produces a more homogenous material. As can be seen in Figure 7d, the EMAA/SBR/asphalt system has more

uniform dispersion and smaller particle size of additives, which presents a better compatibility between binder and additives. Therefore, EMAA are beneficial for the dispersion of SBR modifier, resulting in better mechanical and rheological properties.
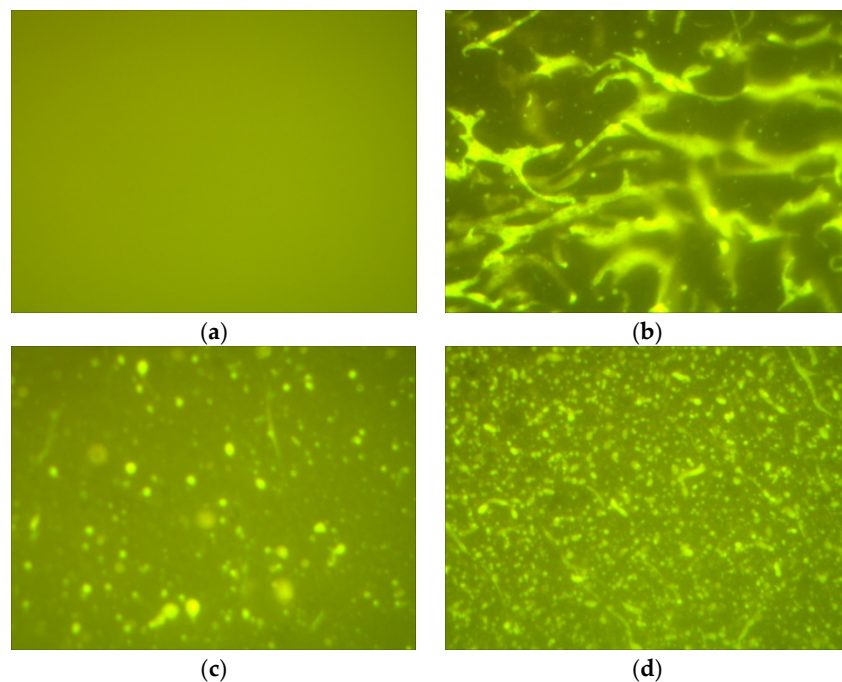
Figure 7. Fluorescence micrographs of different binders: (**a**) Virgin; (**b**) 4%EMAA; (**c**) 3%SBR; (**d**) 4%EMAA/3%SBR.

4.1.5. SEM Test Analysis

The micro morphologies of virgin binder, SBR-modified binder, EMAA/SBR compound-modified binder are presented in Figure 8. The virgin binder appears homogeneous under microscope, as shown in Figure 8a, but the images of SBR-modified binder shows that the SBR polymer disperse as floccules morphology in virgin binder, see Figure 8b. This phenomenon implies the poor stability of SBR-modified binder. The reason is probably because the low molecular oil fraction of binder was absorbed by SBR polymer, which caused the separation between asphaltene and resin. However, the micro morphology of EMAA/SBR compound-modified binder shows that both EMAA particles and SBR disperse uniformly in virgin binder, as seen in Figure 8c. Therefore, when EMAA was added to SBR-modified binder, the small concentration and aggregation of polymer was weakened. The storage stability of EMAA/SBR compound-modified binder improved. Moreover, the interfacial structure between EMAA, SBR polymer, and binder could prevent the movement of macromolecular chains of modified binder, and also lead to the reduction of initiation and propagation of microcracks in binder. Therefore, the anti-fracture property and the mechanical strength of EMAA/SBR compound modified binder improved.
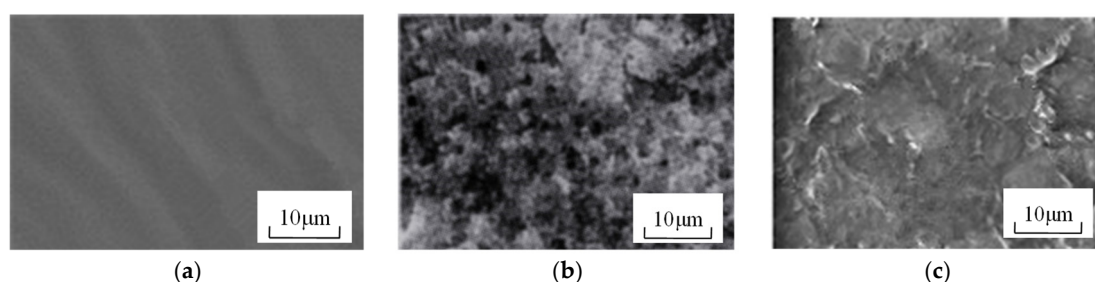

Figure 8. SEM photographs of different binders: (**a**) Virgin; (**b**) 3% SBR; (**c**) 4%EMAA/3%SBR.

4.2. Mixture Testing Results and Discussion

4.2.1. Stiffness—Dynamic Modulus

The average dynamic modulus master curves for different mixtures are shown in Figure 9. Similar to complex modulus of binders, all asphalt mixtures with modified asphalt binders have higher dynamic modulus than the virgin mixture. Generally, the mixtures with EMAA modified binder, including EMAA and EMAA/SBR modification, are stiffer than the other mixtures. For 4% EMAA and 4%EMAA/3%SBR mixtures, the master curves are nearly the same at low frequencies/high temperatures, while the dynamic modulus of 4%EMAA/3%SBR mixture is greater than 4% EMAA mixture at high frequencies/low temperatures. Therefore, 4%EMAA/3%SBR mixture mostly exhibit higher stiffness than 4% EMAA mixture. However, it should be noted that there is no significant difference between these two mixtures. It also can be seen from the master curves of the virgin and 3% SBR mixtures that the dynamic modulus are almost the same at low frequencies/high temperatures, but not for high frequencies/low temperatures.
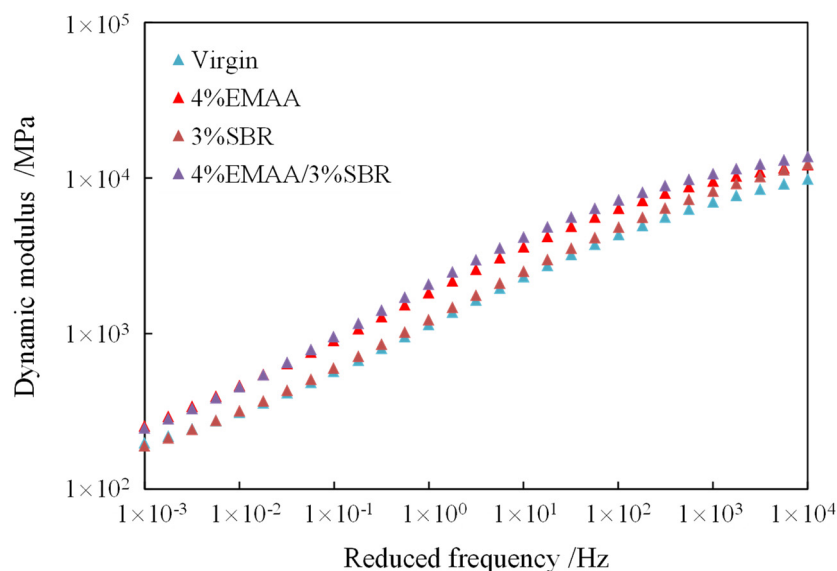
Figure 9. Dynamic modulus master curve for different mixtures.

4.2.2. Relaxation—Phase Angle

Figure 10 shows the phase angle master curves of four kinds of mixtures. Generally, the higher phase angle indicates the better relaxation capability of mixtures, which can be an indicator of better resistance against cracking. The mixtures with modified binders show the higher phase angle values than the virgin mixtures, except for 4% EMAA, indicating that the 4% EMAA mixture may be more prone to cracking. Among all the mixtures, the 4%EMAA/3%SRB and 3%SBR-modified asphalt mixtures show the highest phase angle, which indicates a higher relaxation capacity under a certain load condition. It should be noted that the phase angle is always more variable than dynamic modulus, especially at higher temperatures/lower frequencies.
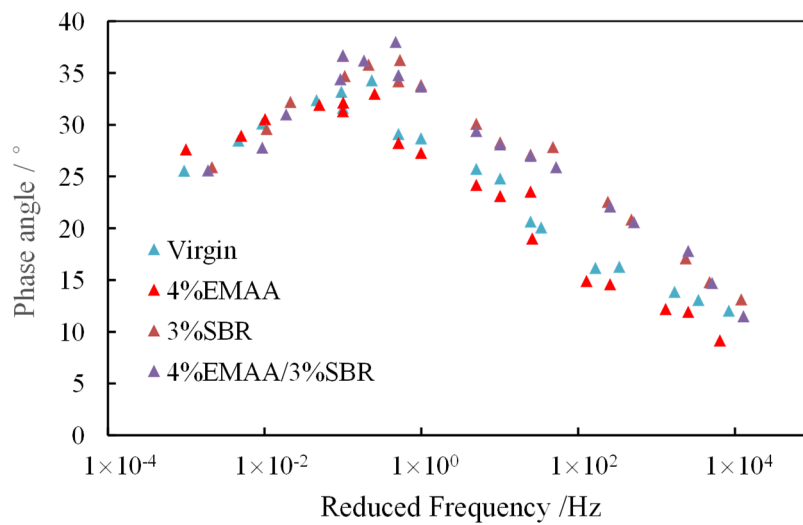
Figure 10. Phase angle of different mixtures.

4.2.3. Cracking Behavior at Low Temperature

The results from TSRST test are presented in Figures 11 and 12, showing the mean values for three replicates. The error bars indicate one standard deviation. As can be seen in Figure 11, fracture temperature of the virgin, 3% SBR, and 4%EMAA/3%SBR mixtures are within a few degrees from −24.0 to −27.2 °C, which does not result in an obvious distinction between these mixtures. The 4% EMAA mixture shows a warmer fracture temperature than the other mixture, indicating that the EMAA may have a negative impact on low-temperature cracking. In addition, based on Figure 12, 4%EMAA mixture ranks the second in fracture stress, which indicates a relatively good low-temperature anti-cracking ability to some extent. Therefore, the fact that the EMAA has an effect on low-temperature cracking properties of asphalt mixture needs further investigation. Based on the results of Figures 11 and 12, 4%EMAA/3%SBR mixture shows the best low-temperature cracking property with the highest fracture stress and second lowest fracture temperature. This is probably related to the compatibility and chemical effects between SBR and EMAA. It is in good agreement with previous studies [37] that found that SBR has a great impact on low-temperature properties of asphalt mixtures.
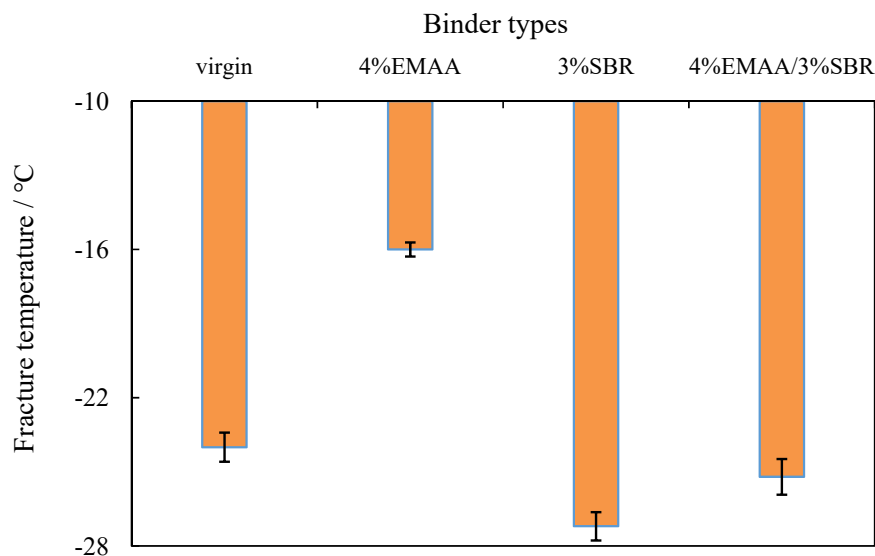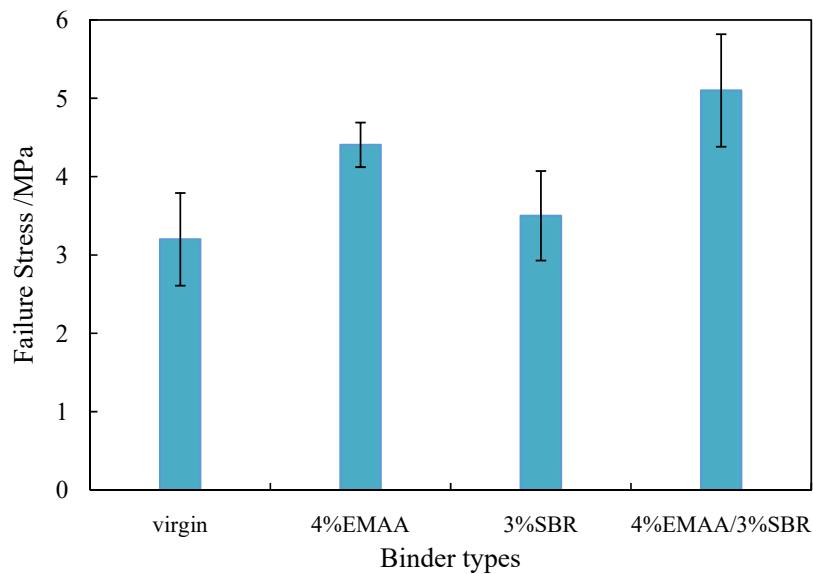

Figure 11. Fracture temperature (thermal stress-restrained specimen test (TSRST)) of different asphalt mixtures.

Figure 12. Failure stress (TSRST) of different asphalt mixtures.

The FST results from DCT test are shown in Figure 13. The FST is obtained as fracture energy (G_f) divided by fracture strength (S_f). It is shown that FST can better characterize the fracture process of asphalt mixture. Among four different mixtures, 4% EMAA mixture has the lowest FST value. It also can be observed from Figure 13 that 4%EMAA/3%SBR mixture evidently shows the highest FST value, which is 32% higher than that of the virgin mixture. Moreover, the variation in FST values as a result of different modification is assessed. As can be seen in Figure 13, the variation of 4%EMAA/3%SBR mixture is only 10.4%. Much higher variations (36.9%, 25.4%, and 14.7%) are observed in the other three mixtures, thus indicating that 4%EMAA/3%SBR mixture shows great homogeneity and integrity compared to the other mixtures.

Overall, it can be concluded from the TSRST and DCT testing methods that adding EMAA has a negative effect on low-temperature behavior of virgin mixtures. However, EMAA/SBR compound modifier could improve the low-temperature property of mixture. The reasons may be the chemical reactions between the two modifiers, as well as the compatibilization of EMAA on SBR-modified asphalt.
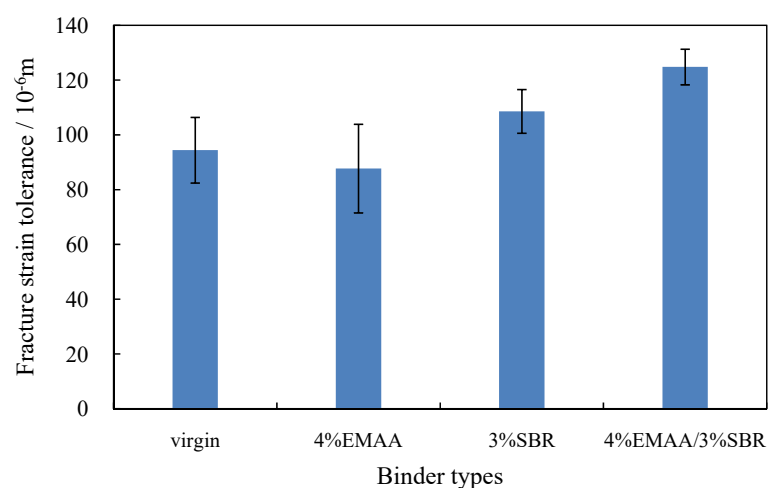
Figure 13. Fracture strain tolerance (disk-shaped compact tension (DCT)) of different asphalt mixtures.

4.2.4. Self-healing Capacity

The fatigue-healing-fatigue test results are shown in Table 7. It can be seen from the number of cycles to failure (N_f) that the ranking of fatigue life under the 0.5 stress ratio is 4%EMAA/3SBR > 3%

SBR > virgin > 4% EMAA, which can reflect the fatigue performance ranking to some degree. Moreover, it can be seen that the fatigue lives ($N_1 + N_2$) of asphalt mixtures increase after the healing. In which, N_1 is the 30% fatigue life of each mixture and N_2 is the full fatigue life of 30% fatigue damage's mixture after 24 h interval in room temperature. This is because the asphalt mixtures can heal themselves through a time interval or under high-temperature conditions. Therefore, the fatigue life of all asphalt mixtures has been extended. In addition, the 4%EMAA/3%SBR mixture has the highest healing rate, which is nearly three times as much as that of the virgin asphalt mixture. However, the mechanism of self-healing still needs investigations.

Table 7. Results of self-healing property of asphalt mixtures.

Asphalt Type	Stress Ratio	N_f/Cycles	N_1/Cycles	N_2/Cycles	($N_1 + N_2$)/Cycles	H/%
Virgin		20,158	6047	16,752	22,799	13.1
4% EMAA		18,596	5578	19,256	24,834	33.5
3% SBR	0.5	31,596	9478	30,456	39,934	26.4
4%EMAA/3%SBR		36,525	10,957	40,258	51,215	40.2

5. Summary and Conclusions

This paper evaluated the effect of EMAA and SBR modifiers on the rheological properties, cracking behavior, self-healing, compatibility, stability, and anti-fracture property of binders, and viscoelastic characteristics, low-temperature cracking, and self-healing properties of asphalt mixtures. The binders were evaluated using complex modulus, Glover–Rowe parameter, self-healing ductility rate, and fluorescence micrographs, and the mixtures were assessed using dynamic modulus, phase angle, fracture temperature, fracture strain tolerance (FST), and self-healing rate. Testing was conducted on the virgin binder, EMAA-modified binder, SBR-modified binder, EMAA/SBR compound-modified binder, and their mixtures. The following conclusions were drawn based on the testing results:

1. The conventional tests, including softening point, equivalent softening point (T800), and kinematic viscosity (135 °C) showed that the contents of 4% EMAA and 3% SBR can increase the physical properties and decrease the costs;

2. 4%EMAA was effective in improving the complex shear modulus of binder. 3%SBR showed little effect on complex shear modulus of asphalt mixtures compared with virgin binder, however it was more effective at high temperatures. The G-R parameter results showed that 4%EMAA has a negative effect on anti-cracking ability of binder. 4%EMAA/3%SBR may show the best anti-cracking ability on site;

3. The ductility test results showed that EMAA had great potential to improve the self-healing behavior of binder, which was more evident in the ductility test of EMAA compound SBR-modified binder. What is more, the EMAA/SBR/asphalt system showed the best homogeneity and compatibility among four kinds of binders based on the fluorescence micrographs. Also, the anti-fracture property and the mechanical strength of EMAA/SBR compound-modified binder improved based on the SEM images. The fatigue–healing–fatigue test results showed that the fatigue life of EMAA/SBR compound-modified mixture had been significantly extended with a 24 h healing interval;

4. The results of dynamic modulus testing showed that the modified asphalt mixtures are stiffer than virgin mixture, while for SBR-modified asphalt mixture, the improvement was not found to be significant. The results of phase angle showed that EMAA had a negative effect on anti-cracking ability. However, the phase angles of EMAA/SBR compound-modified mixture was slightly greater than SBR-modified mixture, indicating better resistance to cracking;

5. According to the results of fracture temperature and fracture stress, the EMAA/SBR compound-modified asphalt showed the best low-temperature cracking resistance. The fracture

strain tolerance (FST) was selected as the parameter instead of fracture energy. The results showed that EMAA/SBR compound-modified mixture had the greatest FST value, indicating the best crack resistance at low-temperatures. In addition, the EMAA/SBR compound-modified mixture had the lowest variability of FST value.

In addition, there are also other tests that can supplement this study, however they were not conducted due to the scope of this study. Such tests may include differential scanning calorimetry (DSC) test and some scratch tests. DSC tests are recommended to show the thermal and chemical stability of different binders. We also recommend doing scratch test to study the abrasive resistance of different mixtures.

References

1. Agzenai, Y.; Pozuelo, J.; Sanz, J.; Perez, I.; Baselga, J. Advanced self-healing asphalt composites in the pavement performance field: Mechanisms at the nano level and new repairing methodologies. *Recent Pat. Nanotechnol.* **2015**, *9*, 43. [CrossRef] [PubMed]

2. Baldino, N.; Gabriele, D.; Rossi, C.O.; Seta, L.; Lupi, F.R.; Caputo, P. Low temperature rheology of polyphosphoric acid (PPA) added bitumen. *Constr. Build. Mater.* **2012**, *36*, 592–596. [CrossRef]

3. Becker, Y.; Méndez, M.P.; Rodríguez, Y. Polymer modified asphalt. *Vis. Tecnol.* **2001**, *9*, 39–50.

4. Zhang, F.; Hu, C. Influence of aging on thermal behavior and characterization of SBR compound modified asphalt. *J. Therm. Anal. Calorim.* **2014**, *115*, 1211–1218. [CrossRef]

5. Kim, Y.R.; Little, D.N.; Lytton, R.L.; D'Angelo, J.; Davis, R.; Rowe, G. Use of dynamic mechanical analysis (DMA) to evaluate the fatigue and healing potential of asphalt binders in sand asphalt mixtures. *J. Assoc. Asph. Paving Technol.* **2002**, *71*, 176–206.

6. Little, D.N.; Lytton, R.L.; Williams, D.; Kim, Y.R. An analysis of the mechanism of microdamage healing based on the application of micromechanics first principles of fracture and healing. *J. Assoc. Asph. Paving Technol.* **1999**, *68*, 501–542.

7. Karki, P.; Li, R.; Bhasin, A. Quantifying overall damage and healing behaviour of asphalt materials using continuum damage approach. *Int. J. Pavement Eng.* **2015**, *16*, 350–362. [CrossRef]

8. Sun, D.; Sun, G.; Zhu, X.; Guarin, A.; Li, B.; Dai, Z.; Ling, J. A comprehensive review on self-healing of asphalt materials: Mechanism, model, characterization and enhancement. *Adv. Colloid Interface Sci.* **2018**, *256*, 65–93. [CrossRef]

9. Qiu, J.; Van de Ven, M.; Wu, S.; Yu, J.; Molenaar, A. Evaluating self healing capability of bituminous mastics. *Exp. Mech.* **2012**, *52*, 1163–1171. [CrossRef]

10. Liu, Q.; Schlangen, E.; van de Ven, M. Induction healing of porous asphalt concrete beams on an elastic foundation. *J. Mater. Civ. Eng.* **2012**, *25*, 880–885. [CrossRef]

11. Dai, Q.; Wang, Z.; Hasan, M. Investigation of induction healing effects on electrically conductive asphalt mastic and asphalt concrete beams through fracturehealing tests. *Construct. Build. Mater.* **2013**, *49*, 729–737. [CrossRef]

12. Apostolidis, P.; Liu, X.; Scarpas, A.; Kasbergen, C.; van de Ven, M. Advanced evaluation of asphalt mortar for induction healing purposes. *Construct. Build. Mater.* **2016**, *126*, 9–25. [CrossRef]

13. Peinado, F.; Medel, E.; Silvestre, R.; Garcia, A. Open-grade wearing course of asphalt mixture containing ferrite for use as ferromagnetic pavement. *Compos. Part B Eng.* **2014**, *57*, 262–268. [CrossRef]

14. Micaelo, R.; Al-Mansoori, T.; Garcia, A. Study of the mechanical properties and selfhealing ability of asphalt mixture containing calcium-alginate capsules. *Construct. Build. Mater.* **2016**, *123*, 734–744. [CrossRef]

15. Li, R.; Zhou, T.; Pei, J. Design, preparation and properties of microcapsules containing rejuvenator for asphalt. *Construct. Build. Mater.* **2015**, *99*, 143–149. [CrossRef]

16. Trask, R.S.; Williams, H.R.; Bond, I.P. Self-healing polymer composites: Mimicking nature to enhance performance. *Bioinspir. Biomim.* **2007**, *2*, 1–9. [CrossRef]

17. Meure, S.; Wu, D.; Furman, S. Polyethylene-co-methacrylic acid healing agents for mendable epoxy resins. *Acta Mater.* **2009**, *57*, 4312–4320. [CrossRef]

18. Meure, S.; Furman, S.; Khor, S. Poly[ethylene-co-(methacrylic acid)] healing agents for mendable carbon fiber laminates. *Macromol. Mater. Eng.* **2010**, *95*, 420–424. [CrossRef]

19. Pingakararwat, K.; Wang, C.; Varley, R.J.; Mouritz, A.P. Self-healing of delamination fatigue cracks in carbon fibre–epoxy laminate using mendable thermoplastic. *J. Mater. Sci.* **2012**, *47*, 4449–4456. [CrossRef]

20. Wang, R.; Wan, C.; Zhang, Y. Study on PE-HD/wood fiber composites compatibilized with ethylene methacrylic acid copolymer. *China Plast.* **2005**, *11*, 63–66.

21. Zhao, B.; Zhao, S.; Zhang, H.; Su, M. Properties and mechanism of composite asphalt modified by nano-$CaCO_3$/SBR. *J. Chang'an Univ.* **2017**, *37*, 15–22.

22. JTG E20-2011. *Standard Test Methods of Bitumen and Bituminous Mixtures for Highway Engineering*; Ministry of Transport of the People's Republic of China: Beijing, China, 2011.

23. JTG F40-2004. *Technical Specification for Construction of Highway Asphalt Pavements*; Ministry of Transport of the People's Republic of China: Beijing, China, 2004.

24. Booshehrian, A.; Mogawer, W.S.; Bonaquist, R. How to construct an asphalt binder master curve and assess the degree of blending between RAP and virgin binders. *J. Mater. Civ. Eng.* **2013**, *25*, 1813–1821. [CrossRef]

25. Glover, C.; Davison, R.; Domke, C.; Ruan, Y.; Juristyarini, P.; Knorr, D.; Jung, S. *Development of a New Method for Assessing Asphalt Binder Durability with Field Evaluation*; Publication FHWA-TX-05-1872-2; National Research Council: Washington, DC, USA, 2005.

26. Aderson, R.M.; King, G.; Hanson, D.; Blankenship, P.B. Evaluation of the Relationship between Asphalt Binder Properties and Non-Load Related Cracking. *J. Assoc. Asph. Paving Technol.* **2011**, *80*, 649–662.

27. Rowe, G.M.; King, G.; Anderson, M. The Influence of Binder Rheology on the Cracking of Asphalt Mixes on Airport and Highway Projects. *J. Test. Eval.* **2014**, *42*, 1063–1072. [CrossRef]

28. Dong, F.; Zhao, W.; Zhang, Y.; Wei, J.; Fan, W.; Yu, Y.; Wang, Z. Influence of SBS and asphalt on SBS dispersion and the performance of modified asphalt. *Constr. Build. Mater.* **2014**, *62*, 1–7. [CrossRef]

29. AASHTO. *TP 10-93, Standard Test Method for Thermal Stress Restrained Specimen Tensile Strength*; Provincial Standards; American Association of State Highway and Transportation Officials (AASHTO): Washington, DC, USA, 1993.

30. Li, X.J.; Marasteanu, M.O. Using semi circular bending test to evaluate low temperature fracture resistance for asphalt concrete. *Exp. Mech.* **2010**, *50*, 867–876. [CrossRef]

31. Al-Qadi, I.; Ozer, H.; Lambros, J.; Khatib, A.; Singhvi, P.; Khan, T.; Rivera, J.; Doll, B. *Testing Protocols to Ensure Performance of High Asphalt Binder Replacement Mixes Using RAP and RAS*; Report No. FHWA-ICT-15-017; Illinois Center for Transportation: Rantoul, IL, USA, 2015.

32. Pérez-Jiménez, F.; Botella, R.; Martínez, A.H.; Miró, R. Analysis of the Mechanical Behaviour of Bituminous Mixtures at Low Temperatures. *Constr. Build. Mater.* **2013**, *46*, 193–202. [CrossRef]

33. Zhu, Y.; Dave, V.E.; Rahbar-Rastegar, R.; Daniel, J.S.; Zofka, A. Comprehensive Evaluation of Low Temperature Fracture Indices for Asphalt Mixtures. *Road. Mater. Pavement Des.* **2017**, *18* (Suppl. 4), 467–490. [CrossRef]

34. Jacues, C.; Daniel, J.S.; Bennert, T.; Reinke, G.; Norouzi, A.; Ericson, C.; Mogawer, W.; Kim, Y.R. Effect of silo storage time on the characteristics of virgin and reclaimed asphalt pavement mixtures. *Transport. Res. Rec.* **2016**, *2573*, 76–85. [CrossRef]

35. Liang, M.; Xin, X.; Fan, W.; Sun, H.; Yao, Y.; Xing, B. Viscous properties, storage stability and their relationships with microstructure of tire scrap rubber modified asphalt. *Constr. Build. Mater.* **2015**, *74*, 124–131. [CrossRef]

36. Hao, P.; Zhai, R.; Zhang, Z.; Cao, X. Investigation on performance of polyphosphoric acid (PPA)/SBR compound-modified asphalt mixture at high and low temperatures. *Road Mater. Pavement Des.* **2019**, *20*, 1376–1390. [CrossRef]

37. Zhang, F.; Yu, J. The research for high-performance SBR compound modified asphalt. *Constr. Build. Mater.* **2010**, *24*, 410–418. [CrossRef]